Structural Engineering and Mechanics, *Vol. 60, No. 5 (2016) 891-902*
DOI: http://dx.doi.org/10.12989/sem.2016.60.5.891

Dynamic responses of a beam with breathing cracks by precise integration method

C.C. Cui, X.S. He, Z.R. Lu, Y.M. Chen* and J.K. Liu

Department of Mechanics, Sun Yat-sen University, Xingang Road West 135, 510275 Guangzhou, China

(Received January 22, 2015, Revised September 21, 2016, Accepted October 6, 2016)

Abstract. The beam structure with breathing cracks subjected to harmonic excitations was modeled by FEM based on Euler-Bernoulli theory, and a piecewise dynamical system was deduced. The precise integration method (PIM) was employed to propose an algorithm for analyzing the dynamic responses of the deduced system. This system was first divided into linear sub-systems, between which there are switching points resulted from the breathing cracks. The inhomogeneous terms due to the external excitations were tackled by introducing auxiliary variables to express the harmonic functions, hence the sub-systems are homogeneous. The PIM was then applied to solve the homogeneous sub-systems one by one. During the procedures, a predictor-corrector algorithm was presented to determine the switching points accurately. The presented method can provide solutions with an accuracy to a magnitude of 10^{-12} compared with exact solutions obtained by the theories of ordinary differential equations. The PIM results are much more accurate than Newmark ones with the same time step. Moreover, it is found that the PIM can maintain a high level of accuracy even when the time step increases within a relatively wide range.

Keywords: beam; breathing crack; precise integration method; switching point

1. Introduction

The influences and detections of cracks on beam structures have stimulated the curiosities and interests of many researchers and engineers for decades (Chondros, Dimarogonas *et al*. 2001, Kim and Stubbs 2003, Kisa and Brandon 2000, Krawczuk 2002, Law and Zhu 2004, Kisa 2012). As we know, vibration analysis of a cracked beam focused mainly on direct simulations based on FEM (Krawczuk 2002, Shakti *et al*. 2015) as well as modal analysis (Kim and Stubbs 2003). A variety of dynamical behaviors were reported by time-marching integration techniques. It is very useful for the better understanding of the dynamic nature of the beam structures (Akbas and Seref 2016). More importantly, they can provide much useful information for crack identifications (Andreaus and Baragatti 2009, Moradi, Razi *et al*. 2011, Abolbashari *et al*. 2014). Many studies demonstrated that a crack in a beam may cause the structure to exhibit nonlinear dynamical behaviors, if the crack opens and closes during the vibration, which actually indicates a breathing crack (Lee and Fenves 1998, Andreaus, Batra *et al*. 2005, Andreaus, Casini, *et al*. 2007). Breathing cracks have received continuous attentions usually with emphasis on the implications to vibration features as

*Corresponding author, Professor, E-mail: chenymao@mail.sysu.edu.cn

http://www.techno-press.org/?journal=sem&subpage=8 ISSN: 1225-4568 (Print), 1598-6217 (Online)

well as crack detections (Ariaei, Ziaei-Rad *et al*. 2009, Bouboulas and Anifantis 2011, Caddemi, Calio *et al*. 2010, Andreaus and Baragatti 2012).

Real time simulation is one of the pivotal tasks for dynamics research. As for a cracked beam, specifically, the time-marching integration is usually implemented using the Newmark method, the Wilson method, and the Runge-Kutta method etc (Wang, Lu *et al*. 2012, Ozkul 2004). These techniques are both unconditionally stable and can provide very accurate results as long as the time step is refined enough. However, the accuracy is usually improved at the expense of tremendous computational resources.

On the other hand, there should be a criterion for the judgment whether the breathing crack opens or closes during numerical simulations. This criterion will lead to switching points (Law and Zhu 2004). Though the switching points can be approximated very accurately as the time step is chosen small enough, the computational cost is very high even unacceptable in some working conditions such as real time structural health monitoring as well as damage detections. Therefore, it is worthy of proposing some more efficient approaches to tackle this problem.

A simple yet efficient algorithm, named as precise integration method (PIM), was initiated by Zhong and Williams (1994) two decades ago. The most outstanding merit of PIM consists in its high precision and efficiency. Theoretically, it can reach computer precision without too much computational costs. It is also applicable to both initial-valued and boundary-valued problems (Huang, Deng *et al*. 2007, Zhang and Huang 2013). So far, the PIM has been developed and applied in various computational problems such as dynamical systems, wave propagation, optimal control, structural mechanics, electro-magnetic wave guide problems, bio-medical engineering problems, aeroelastics, and soil mechanics, etc (Zhong 2004, Cui, Liu *et al.* 2015, Gao, Wu *et al*. 2012, Wang 2011, Lin, Han *et al*. 2013).

In this study, the PIM will be applied to solve the dynamical equations of a beam with breathing cracks subjected to external harmonic excitations. The beam is modeled by the Euler-Bernoulli beam theory based on FEM. An alternative approach could be the Meshless Local Petrov-Galerkin Method (Andreaus, Batra *et al*. 2005). Under the assumption that an opening crack can cause a reduction of the stiffness (Abdel Wahab, De Roeck *et al*. 1999), a piecewise dynamical system is deduced. The system is further separated as linear sub-systems, between which there are switching points. The PIM is then used to solve the sub-systems repeatedly. During the computation, a predictor-corrector algorithm is proposed based on the PIM to accurately determine the switching points.

2. Equations of motions

Figure 1 presents a simply supported beam with a breathing crack at its bottom edge of the mid-point. The parameters for the beam are chosen as follows: the stiffness as EI=5625 KN/m, the density as ρ=7850 kg/m^3, and the length as L=3 m. As an illustration, the beam is modeled as an Euler-Bernoulli beam and is divided into 20 elements. Each element has two nodes. The nodes are numbered consecutively from left to right, with the two supports as Node-1 and Node-21, respectively. Each node has two degrees-of-freedom. The vertical and angular displacement are denoted as v and θ, respectively.

The breathing crack locates at Element-10, with two nodes as Node-10 and Node-11. There are many theoretical as well as experimental treatments of a breathing crack, for example, modeling the breathing crack as a reduction of stiffness (Abdel Wahab, De Roeck *et al*. 1999, Sinha, Friswell

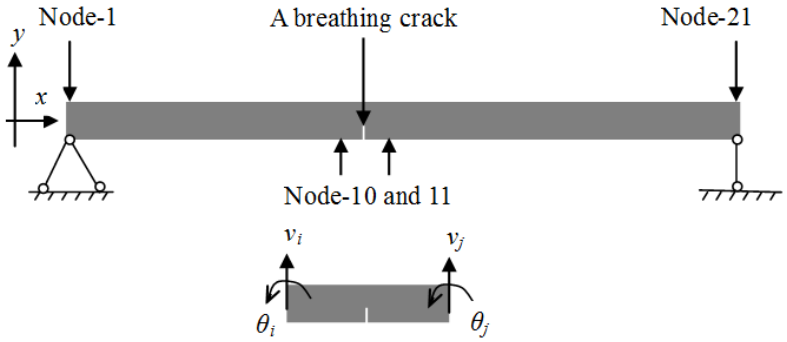

Fig. 1 A simply supported beam with a breathing crack

et al. 2002), or as a frictional contact problem (Bouboulas and Anifantis 2011), etc. The first strategy will be employed in this study.

Assume the crack only influences the element that it is located at, i.e., Element-10. It reduces to ηEI at Element-10 as the crack opens, with $0<\eta<1$ as the reduction ratio. When the crack closes, the element stiff matrix for the damaged element is K_{10}. It becomes ηK_{10} as the crack opens. For convenience, we rewrite the corresponding stiffness matrix as $\overline{K}_{10} = \eta K_{10}$. According to the Euler-Bernoulli beam theory, the longitudinal strain is assumed as 0 at the mid-plane of the beam, i.e., $\varepsilon_x=0$ if $y=0$. The crack opens if $\varepsilon_x>0$ at the upper side of the mid-plane, i.e., $y>0$, otherwise it closes. Additionally, the longitudinal strain at Element-10 can be approximated as

$$\varepsilon_x = -y\frac{\partial^2 v}{\partial^2 x} = -y\frac{\partial \theta}{\partial x} \approx -y\frac{\theta_{11}-\theta_{10}}{l_{ij}} \tag{1}$$

Mathematically, the crack opens when $\theta_{10}>\theta_{11}$, otherwise it closes.

A harmonic external force, $f\cos(\omega t)$, acts on the beam at 1.35 m from the left side of the beam, i.e., at Node-10. The harmonically forced responses can be applied in crack identifications (Andreaus and Baragatti 2011). The equations of motions can be deduced as

$$M\ddot{x} + C\dot{x} + Kx = f\cos(\omega t) \tag{2}$$

where the displacement is $x=[\theta_1,v_2,\theta_2,...,v_{20},\theta_{20},\theta_{21}]^T$ (with $v_1=v_{21}=0$). The superscript denotes the differentiation with respect to time t. Here, M and C are time-invariant mass and damping matrixes, respectively. The stiffness matrix, K, depends upon the displacement and is assembled by the element stiffness matrixes as follows

$$K = \begin{cases} \sum_{i=1}^{20} K_i, & x_{19} \le x_{21} \\ \sum_{i=1,i\neq 0}^{20} K_i + \eta K_{10}, & x_{19} > x_{21} \end{cases} \tag{3}$$

3. Precise integration method

The first-order angular frequency of the free vibration is ω_1=240rad/s. Under the transformation of a non-dimensional time scale as $\tau=\omega_1 t$, Eq. (2) becomes

$$\omega_1^2 Mx'' + \omega_1 Cx' + K(x)x = f\cos(\overline{\omega}\tau) \tag{4}$$

The superscript denotes differentiation with τ, and $\overline{\omega} = \omega/\omega_1$. Denote $y = [x, x']^T$, and rewrite Eq. (4) as a system of first-order ordinary differential equations as

$$y' = \begin{cases} A_1 y + F\cos(\overline{\omega}\tau), & y_{19} \le y_{21} \\ A_1 y + F\cos(\overline{\omega}\tau), & y_{19} > y_{21} \end{cases}$$

$$A_i = \begin{bmatrix} 0 & I \\ -\frac{1}{\omega_1^2}M^{-1}K_i & -\frac{1}{\omega_1}M^{-1}C \end{bmatrix}, F = -\frac{1}{\omega_1^2}M^{-1}\begin{bmatrix} 0 \\ f \end{bmatrix}, \tag{5}$$

with its dimension as 80 which is two times of the dimension of x (i.e., 40). In order to eliminate the inhomogeneous terms, a dimension expansion method is employed (Gu, Chen *et al*. 2001). We introduce two new variables $y_{81} = \cos(\overline{\omega}\tau)$ and $y_{82} = \sin(\overline{\omega}\tau)$ satisfying

$$y'_{81} = -\overline{\omega} y_{82}, y'_{82} = \overline{\omega} y_{81} \tag{6}$$

Synthesizing Eqs. (5)-(6) results into

$$y' = B_i y$$

$$B_i = \begin{bmatrix} 0 & I & 0 & 0 \\ -\frac{1}{\omega_1^2}M^{-1}K_i & -\frac{1}{\omega_1}M^{-1}C & \frac{1}{\omega_1^2}M^{-1}f & 0 \\ 0 & 0 & 0 & -1 \\ 0 & 0 & 1 & 0 \end{bmatrix}, y = \begin{bmatrix} x \\ x' \\ y_{81} \\ y_{82} \end{bmatrix} \tag{7}$$

where B_i is the coefficient matrix for sub-system i (i=1or 2). In each sub-system, the analytical solution of Eq. (7) can be given as

$$y = \exp(B_i\tau)y(0) \tag{8}$$

with $y(0)$ as an initial condition with $y_{81}(0)$=1 and $y_{82}(0)$=0. A time step, $\Delta\tau$, is chosen repeatedly to generate solutions for a given time series, denoted as [0, $\Delta\tau$, 2$\Delta\tau$, …, $N\Delta\tau$]. Note that the exponent matrix, exp($B_i\Delta\tau$), holds that exp($nB_i\Delta\tau$)=[exp($B_i\Delta\tau$)]^n. At the n-th time point, the solution can be given as $y^n = [\exp(B_i\Delta\tau)]^n y(0)$.

In PIM, the small time step, $\Delta\tau$, is further split uniformly as $\delta=\Delta\tau/2^m$ with m as an positive integer as 20 or larger. By this means, the exponential matrix can be calculated recursively by

$$T = \exp(B_i\Delta\tau) = \exp(B_i\Delta\tau/2^m)^{2^m} \tag{9}$$

Expanding exp($B_i\delta$) as a series and retaining several lower-order terms, we have

$$\exp(B_i\Delta\tau/2^m) = I + B_i\delta + (B_i\delta)^2/2 + (B_i\delta)^3/6 + (B_i\delta)^4/24 = I + T_a \tag{10}$$

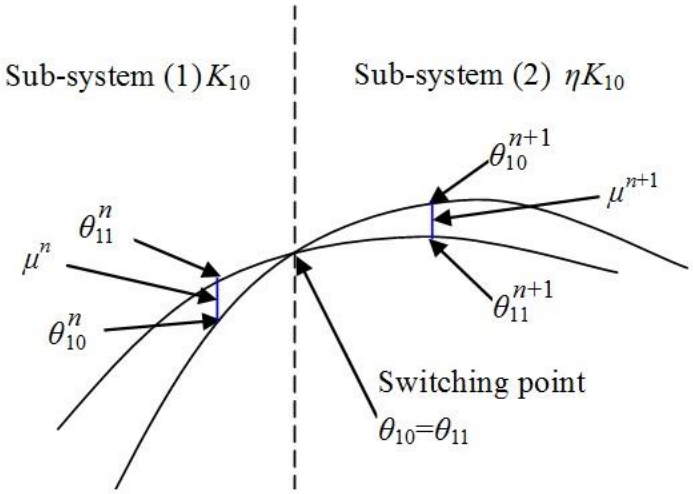

Fig. 2 Illustration of the predictor-corrector algorithm for seeking a switching point

The matrix T_a is introduced to distinguish the higher-order terms from I. Substitution of Eq. (10) into (9) results in

$$T = (I + T_a)^{2^m} = (I + T_a)^{2^{m-1}} \times (I + T_a)^{2^{m-1}} \tag{11}$$

The factorization should be iterate m times, for instance, we can let the index iter increase from iter=0 to iter=m stepwise, and in each iteration step carry out the calculation to matrix T_a by $T_a=2T_a+T_a\times T_a$. After these iterations, the exponential matrix for one step ($\Delta\tau$) can finally be given as $T=I+T_a$. More details about solving the exponential matrix for the above procedures can be referred to Zhong (2004).

4. Determine switching points

Note that all the above PIM procedures are based on the assumption that, the vibration state $y^n=y(n\Delta t)$ and its following state $y^{n+1}=y((n+1)\Delta t)$ both locate at either one of the sub-systems. Generally, the state will finally leave one sub-system to another as θ_{10}-θ_{11} passes 0. That means a switching point, as shown in Fig. 2. It is necessary to point out that, y^{n+1} is calculated from y^n under the assumption that the curve between them is totally located at sub-system (1).

A predictor-corrector algorithm will be presented to accurately find the state passing the switching points. If the state is exactly at the switching point, we have $\mu^n=0$ with $\mu^n=\theta_{10}{}^n-\theta_{11}{}^n$. Introduce a mean of ratio

$$\lambda = \frac{\mu^n}{\mu^n - \mu^{n+1}} \tag{12}$$

If y^{n+1} is exactly located at the switching point, the ratio is equal to 1. It is predicted that it needs about $\lambda\Delta\tau$ for y^n reaching the switching point. Then, the predicted state is further corrected as

$$y^{n+1} = \exp(B_i \lambda \Delta\tau) y^n = T^{\lambda} y^n \tag{13}$$

The predictor-corrector algorithm is constructed by repeating Eqs. (12) and (13) until λ approaches 1 closely enough. In this study, the tolerance error between λ and 1 is chosen as 10^{-14}. The effectiveness of the presented algorithm will be validated by numerical results.

5. Numerical examples

5.1 A simply supported beam with a breathing crack

The first two free vibration frequencies of the intact beam are 38.26 Hz and 154.5 Hz obtained with N=20 elements. Frequency reduction in elastic beams due to a stable crack is dealt with by Andreaus (2003). The obtaned frequencies agree well with the exact ones (38.15 Hz and 152.6 Hz). As an illustrative example, we take the excitation frequency as ω=200 rad/s and f=100 KN. And the reduction ratio of stiffness is chosen as η=0.8. The non-dimensional frequency in Eq. (5) is given as $\overline{\omega} = 200/\omega_1 = 0.8333$. Fig. 3 shows the time histories for θ_{10} and θ_{11}, respectively. The integration begins with the initial conditions as $y(0)$=0 except that $y_{81}(0)$=1. No matter the time step is chosen as small ($\Delta\tau$=0.1), relatively large ($\Delta\tau$=0.5) or very large ($\Delta\tau$=1), the PIM results are in nice agreement with Newmark solutions with $\Delta\tau$=0.01. In addition, the switching points indicated by the intersecting points can be determined for all three time steps.

Accurate and efficient determination of the switching points between sub-systems is very helpful for accurate and efficient numerical simulations. Table 1 shows two numerical cases for

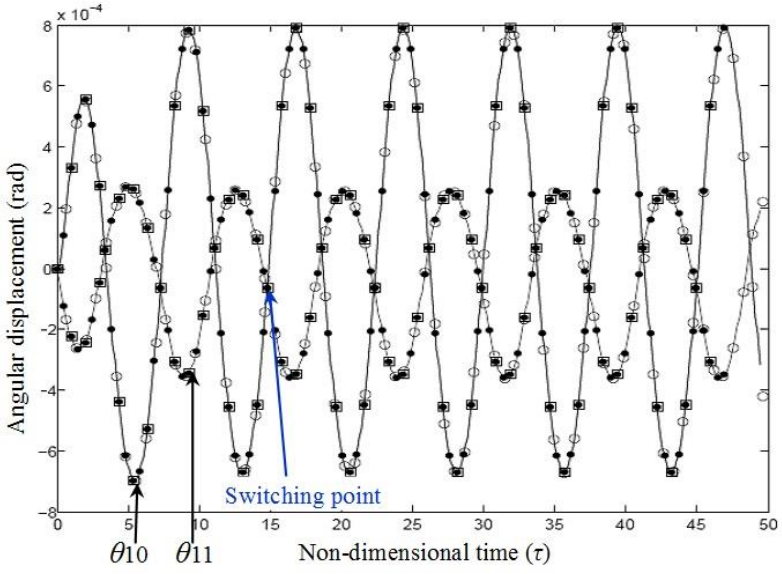

Fig. 3 Time histories for angular displacements θ_{10} and θ_{11}, respectively. The squares, solid dots and solid lines denote PIM results with $\Delta\tau$=1, 0.5, 0.1, respectively. The circlets represent Newmark solutions with $\Delta\tau$=0.01

Table1 Switching points found by the predictor-corrector algorithm

θ_{10}	θ_{11}	Ratio (λ)	Repeats
$\Delta\tau$=0.1 (Sub-system 2 switches to Sub-system 1)			
0.963478307099378e-4	0.444384128241526e-4	τ=3.3	
0.473150960462384e-4	0.644947824331599e-4	0.751340148815502	0
0.596355585755368e-4	0.595209055461572e-4	1.002213602662304	1
0.595539847620296e-4	0.595539792349865e-4	1.000000106474776	3
0.595539808295935e-4	0.595539808293272e-4	1.000000000005130	5
0.595539808294030e-4	0.595539808294049e-4	0.999999999999963	6
$\Delta\tau$=1 (Sub-system 1 switches to Sub-system 2)			
-0.529853453049430e-3	0.135185008316945e-3	τ=6.37529918460170	
-0.349009848623553e-4	-0.740323736301208e-4	0.944429048246938	0
-0.661855157974566e-4	-0.625343027001704e-4	1.005520537486687	1
-0.635212395921967e-4	-0.635208785463006e-4	1.000000542895055	5
-0.635209760886156e-4	-0.635209760531082e-4	1.000000000053391	9
-0.635209760627096e-4	-0.635209760626985e-4	1.000000000000017	13

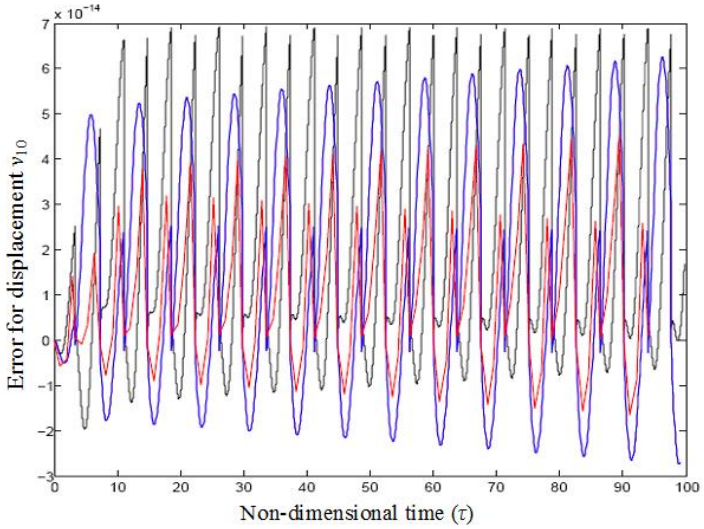

Fig. 4 Absolute errors for v_{10} obtained by PIM for $\Delta\tau$=0.01 (black), $\Delta\tau$=0.1 (blue), and $\Delta\tau$=1 (red) versus that for $\Delta\tau$=0.001

switching points obtained by the predictor-corrector algorithm. As one can see, the ratio defined by Eq. (12) converges rapidly to 1 for both the cases of $\Delta\tau$=0.1 and $\Delta\tau$=1, respectively. That implies the switching points can be approximated very accurately and efficiently. Though more calculations are needed as $\Delta\tau$ increases, the repeated calculations only doubles as $\Delta\tau$ increases by one order of magnitude. It is reasonable to say the presented approach is computationally efficient.

In order to analyze the influences of the time step on the precision of PIM, we present in Fig. 4 the absolute errors for the displacement at Node-10 (v_{10}) obtained by PIM with $\Delta\tau$=0.01, $\Delta\tau$=0.1,

Table 2 Comparisons between the CPU running times of the PIM, Newmark and exact solutions over [0, 100]

	Time (second, $\Delta\tau$=1)	Time (second, $\Delta\tau$=0.1)	Time (second, $\Delta\tau$=0.01)
PIM	0.1594	0.3947	3.9302
Newmark	0.1949	0.1231	3.6201
Exact	495.6	511.2	543.4

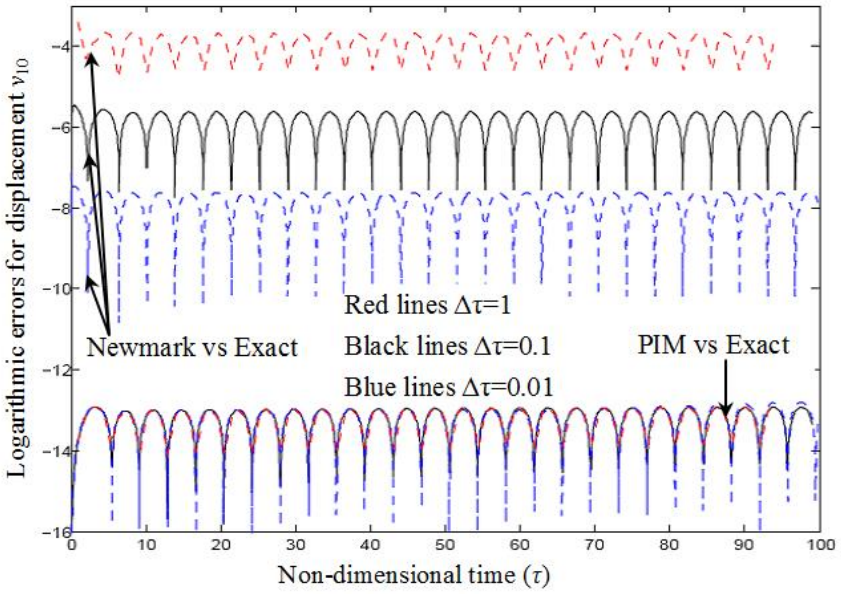

Fig. 5 Logarithmic absolute errors for the displacement at Node-10 (v_{10}) obtained by PIM, Newmark method versus exact solution

and 1, respectively, and compare these solutions with the results obtained with $\Delta\tau$=0.001. Interestingly, the discrepancies between them are at an order of magnitude between 10^{-13} and 10^{-14}. It implies that, the calculation precision can maintain at a high magnitude even as the time step increases in a reasonable range.

Note that, the error also oscillates with the same period as that of the displacement. That is because the difference of the vibration amplitude implies that, there is error in both the maximum and minimum displacements. If the amplitude obtained by PIM is larger than that by exact solution, the maximum displacement by PIM is also larger, whereas the minimum one by PIM is smaller than the counterpart by exact solution.

Next, we will discuss the efficiency and precision of the PIM and Newmark method, respectively, based on exact solutions. The exact solutions of Eq. (5) with given initial conditions are obtained by using the theories of ordinary differential equations. As all sub-systems are linear, analytical expressions can be determined for the solution at each sub-system as long as the initial conditions is given. As the B_i is a coefficient matrix of dimension 82, there are 82 general solutions expressed by exponential functions in the product of the eigenvalues and τ. In order to express all 82 unknowns (y), as many as 82×82 coefficients have to be solved from a linear algebraic

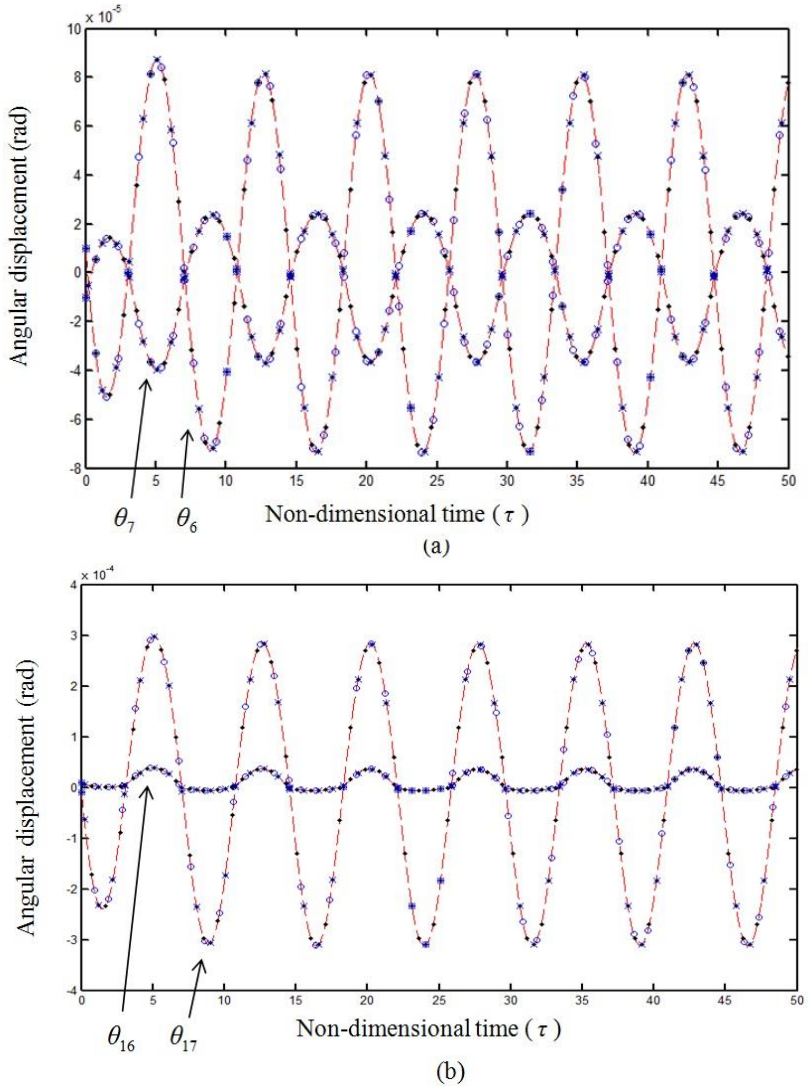

Fig. 6 Time histories for angular displacements θ_6, θ_7, θ_{16} and θ_{17}, respectively. The circlets, solid dots and crosses denote PIM results with $\Delta\tau$=1, 0.5, 0.1, respectively. The red dash lines represent Newmark solutions with $\Delta\tau$=0.01.

equation. Moreover, these coefficients have to be tediously updated when the solution passes a switching point. Considering that these computations will be too time-consuming, we re-divide the beam as only 4 elements as a simple illustration. The CPU running times for the PIM, the Newmark and the exact solutions are shown in Table 2, respectively. The times for PIM are at the same order of magnitude with that for Newmark method. This table also shows the PIM can provide solutions as accurate as the exact solution with much less computational effort.

The respective accuracy of the PIM and Newmark results versus exact solutions are plotted in Fig. 5. The precision of PIM result remains the same as the time step increases. This is an outstanding merit that one can raise time step without losing precision, for instance only the long

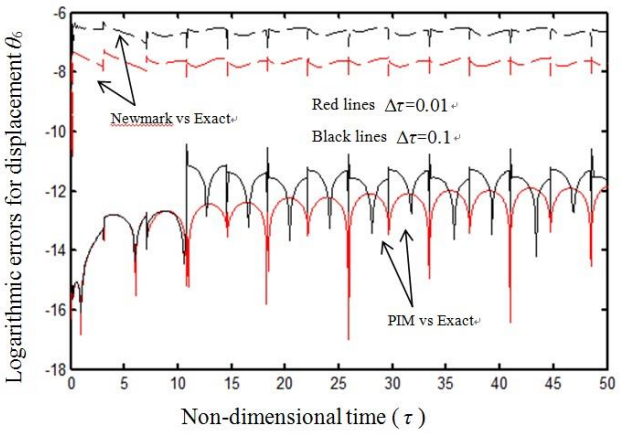

Fig. 7 Logarithmic absolute errors for the displacement at Node-6 (θ_6) obtained by PIM, Newmark method versus exact solution

term vibration responses are needed, or when steady responses such as periodic responses and limit cycle oscillations are interested in. As for the Newmark results, as the time step increases from 0.01 to 0.1 and 1 step by step, the absolute errors increase by two orders of magnitude for each incremental step. It should be pointed out that the exact responses for (v_{10}) are at the order of 10^{-3}. Therefore, the relative error for the Newmark results obtained with $\Delta\tau$=1 increases to about 10%.

5.2 A multi-span continuous beam with multiple breathing cracks

As for the case of a two-span continuous beam with two breathing cracks, the total length of the beam is 3 m and the beam is divided into 20 elements. Two cracks locate at each span of the beam, to be exact, at Element-6 and Element-16, respectively. The harmonic external force is applied to the beam at Node-15. The system should be divided into four linear sub-systems, depending on the states of the two cracks.

Figure 6(a) shows the time histories for θ_6 and θ_7, and (b) the time histories for θ_{16} and θ_{17}, respectively. Nice agreement between the PIM solutions and Newmark ones can also be observed. And Fig. 7 shows the respective accuracy of the PIM and Newmark results versus exact solutions. Though the precision of PIM result tends to decreases slightly as the time step increasing, but the PIM result with a large time step ($\Delta\tau$=0.1) is much more accurate than the results obtained by Newmark method even with a smaller time step ($\Delta\tau$=0.01).

6. Conclusions

We have presented an efficient and highly precise approach, based on the precise integration method (PIM), for the time-marching numerical integration of the dynamic system of a beam with breathing cracks. The beam is modeled using the FEM on the basis of the Euler-Bernoulli beam theory. The piecewise-linear system is separated into linear sub-systems. The switch points between sub-systems can be determined accurately and efficiently by a predictor-corrector

algorithm. With the help of this algorithm, the PIM provides numerical results with very high accuracies. More importantly, the PIM can keep the high accuracy even when the time step increases to relatively large values. With such high precision and efficiency, we could expect the presented method be applicable in structural dynamics simulation of large structures.

Acknowledgements

This work is supported by the National Natural Science Foundation of China (11272361, 11572356, 11672337).

References

Abdel Wahab, M.M., De Roeck, G. and Peeters, B. (1999), "Parameterization of damage in reinforced concrete structures using model updating", *J. Sound Vib.*, **228**(4), 717-30.

Akbas and Doguscan, S. (2016), "Analytical solutions for static bending of edge cracked micro beams", *Struct. Eng. Mech.*, **59** (3), 579-599.

Andreaus ,U. and Baragatti, P. (2009), "Fatigue crack growth, free vibrations and breathing crack detection of Aluminium Alloy and Steel beams", *J. Strain Analysis for Eng. Design*, **44**(7), 595-608.

Andreaus, U. and Baragatti, P. (2011), "Cracked beam identification by numerically analysing the nonlinear behaviour of the harmonically forced response", *J. Sound Vib.*, **330** (4), 721-742.

Andreaus, U. and Baragatti, P., (2012), "Experimental damage detection of cracked beams by using nonlinear characteristics of forced response", *Mech. Syst. Signal Process*. **31**(8), 382- 404.

Andreaus, U., Batra, R.and Porfiri, M. (2005), "Vibrations of Cracked Euler-Bernoulli Beams using Meshless Local Petrov-Galerkin (MLPG) Method", *Comput. Model. Eng. Sci.* (CMES), **9**(2), 111-131.

Andreaus, U., Casini, P. and Vestroni, F. (2003), "Frequency reduction in elastic beams due to a stable crack: numerical results compared with measured test data", *Eng. Trans.*, **51**(1), 1-16.

Andreaus, U., Casini, P. and Vestroni, F. (2005), "Nonlinear features in the dynamic response of a cracked beam under harmonic forcing", *Proc. of DETC'05, 2005 ASME International Design Engineering Technical Conferences and Computers and Information in Engineering Conference*, Long Beach, California, USA, September.

Andreaus, U., Casini, P. and Vestroni, F., (2007), "Nonlinear Dynamics of a Cracked Cantilever Beam Under Harmonic Excitation", *Int. J. Nonlin. Mech.*, **42**(3), 566-575.

Ariaei, A., Ziaei-Rad, S. and Ghayour, M. (2009), "Vibration analysis of beams with open and breathing cracks subjected to moving masses", *J. Sound Vib.*, **326**(3-5), 709-724.

Bouboulas, A.S. and Anifantis, N.K. (2011), "Finite element modeling of a vibrating beam with a breathing crack: observations on crack detection", *Struct. Health Monitoring, Int. J.*, **10**(2), 131-145.

Caddemi, S., Calio, I. and Marletta, M. (2010), "The non-linear dynamic response of the Euler-Bernoulli beam with an arbitrary number of switching cracks", *Int. J. Non-linear Mech.*, **45**(7), 714-726.

Chondros, T.G., Dimarogonas, A.D. and Yao, J. (2001), "Vibration of a beam with a breathing crack", *J. Sound Vib.*, **239** (1), 57-67.

Cui, C.C., Liu, J.K. and Chen, Y.M. (2015), "Simulating nonlinear aeroelastic responses of an airfoil with freeplay based on precise integration method", *Commun. Nonlin. Sci. Numer. Simulat.*, 22, 933-942.

Gao, Q., Wu, F., Zhang, H.W., Zhong, W.X., Howson, W.P. and Williams, F.W. (2012), "A fast precise integration method for structural dynamics problems", *Struct. Eng. Mech.*, **43**(1), 1-13.

Gu, Y.X., Chen, B.S., Zhang, H.W. and Guan, Z.Q. (2001), "Precise time-integration method with dimensional expanding for structural dynamic equations", *AIAA J.*, **39**(12), 2394-2399.

Hossein, A.M., Foad, N. and Soltani, R.J. (2014), "A multi-crack effects analysis and crack identification in

functionally graded beams using particle swarm optimization algorithm and artificial neural network", *Struct. Eng. Mech.*, **51**(2), 299-313.
Huang, Y., Deng, Z.C. and Yao, L.X. (2007), "An improved symplectic precise integration method for analysis of the rotating rigid-flexible coupled system", *J. Sound Vib.*, **299**(1-2), 229–246.
Jena, S.P., Parhi, D.R. and Mishra, D. (2015), "Comparative study on cracked beam with different types of cracks carrying moving mass", *Struct. Eng. Mech.*, **56** (5), 797-811.
Kim, J.T. and Stubbs, N. (2003), "Crack detection in beam-type structures using frequency data", *J. Sound Vib.*, **259** (1), 145-160.
Kisa, K. and Brandon, J. (2000), "The effects of closure of cracks on the dynamics of a cracked cantilever beam", *J. Sound Vib.*, **238** (1), 1-18.
Kisa, M. (2012), "Vibration and stability of axially loaded cracked beams", *Struct. Eng. Mech.*, **44**(3), 305-323.
Krawczuk, M. (2002), "Application of spectral beam finite element with a crack and iterative search technique for damage detection", *Finite Elements Anal. Design*, **38**(6), 537-548.
Law, S.S. and Zhu, X.Q. (2004), "Dynamic behavior of damaged concrete bridge structures under moving vehicular loads", *Eng. Struct.*, **26**(9), 1279-1293.
Lee, J. and Fenves, G.L. (1998), "Plastic-damage model for cyclic loading of concrete structures", *J. Eng. Mech. ASCE*, **124**(8), 892-900.
Lin, G., Han, Z.J., Zhong, H. And Li, J.B. (2013), "A precise integration approach for dynamic impedance of rigid strip footing on arbitrary anisotropic layered half-space", *Soil Dyn. Earthquake Eng.*, **49**, 96-108.
Moradi, S., Razi, P. and Fatahi, L. (2011), "On the application of bees algorithm to the problem of crack detection of beam-type structures", *Comput. Struct.*, **89** (23-24), 2169-2175.
Ozkul, T.A. (2004), "A finite element formulation for dynamic analysis of shells of general shape by using the Wilson-θ method", *Thin-Walled Struct.*, **42**(4), 497-513.
Sinha, J.K., Friswell, M.I. and Edwards, S. (2002), "Simplified models for the location of cracks in beam structures using measured vibration data", *J. Sound Vib.*, **251**(1), 13-38.
Wang, M.F. (2011), "Reduced-order precise integration methods for structural dynamic equations", *Int. J. Numer. Meth. Biomed. Eng.*, **27**(10), 1569-1582.
Wang, W.J., Lu, Z.R. and Liu, J.K. (2012), "Time-frequency analysis of a coupled bridge-vehicle system with breathing cracks", *Int. Multis. Mech.*, **5**(3), 169-185.
Zhang, W.Z. and Huang, P.Y. (2013), "Precise integration method for a class of singular two-point boundary value problems", *Acta Mech. Sin.*, **29**(2), 233-240.
Zhong, W.X. (2004), "On precise integration method", *J. Comput. Appl. Math.*, **163**(1), 59-78.
Zhong, W.X. and Williams, F.W. (1994), "A precise time step integration method", *Proc. Inst. Mech. Eng.*, **208**, 427–430.

CC